Asian Journal of Chemistry; Vol. 34, No. 9 (2022), 2424-2430

ASIAN JOURNAL OF CHEMISTRY

https://doi.org/10.14233/ajchem.2022.23975

A Comparative Study of Macrocyclic Mn(II) Nanocomplex Synthesized Using Sonication-Assisted and Conventional Methods for Biomedical Applications

MEENAKSHI PATYAL[1], KIRANDEEP KAUR[1], NIDHI GUPTA[1], ASHOK KUMAR MALIK[1,*] and KAMALDEEP PAUL[2]

[1]Department of Chemistry, Punjabi University, Patiala-147002, India
[2]School of Chemistry and Biochemistry, Thapar Institute of Engineering and Technology, Patiala-147004, India

*Corresponding author: E-mail: malik_chem2002@yahoo.co.uk

Received: 20 June 2022; *Accepted*: 25 July 2022; *Published online*: 19 August 2022; AJC-20942

Macrocyclic ligand, (7,18-diamino-7,8,17,18-tetrahydrodibenzo[b,j][1,4,9,12]tetraazacyclohexadecine-6,9,16,19(5*H*,10*H*,15*H*,20*H*)-tetraone) and its Mn(II) complex was synthesized *via* sonochemical and conventional methods in nano dimension of 42.29 and 85.63 nm, respectively. The quantitative and qualitative analyses have been done using Fourier Transform Infrared (FTIR), ultraviolet-visible (UV-Vis), mass, electron spin resonance (ESR) spectroscopies and elemental (CHN) analyses. Powder X-ray diffraction (PXRD) and field emission scanning electron microscopy (FE-SEM) have been used for the crystallographic and morphological analyses of the synthesized nano complex, respectively. Based on these studies, octahedral geometry and hexagonal unit cell structure have been proposed for the synthesized Mn(II) nanocomplex. The nano complexes of transition metal can be introduced as the effective nano metal based antimicrobial drugs as they do not require encapsulating or solubilizing chemicals and further offer less side effects and low toxicity as well as improved antimicrobial efficiency. So, it is the need of the hour to work upon such nano based transition metal drugs. The purity, yield and crystallinity of nano complex synthesized by the sonochemical method were found to be far better than those synthesized by the conventional method. The nanocomplex synthesized using two different protocols were screened for *in vitro* against pathogenic bacteria and fungal species by a two-fold serial dilution method and antioxidant studies were as done using the DPPH scavenging method indicating the better and enhanced performance of the nanocomplex obtained using sonication-assisted method. The sonochemical method enhances the properties of the complex by effectively regulating and reducing the size of the nanocomplex and hindering their agglomeration and has better biomedical applications in comparison to conventional methods.

Keywords: Tetraazacyclo macrocyclic ligand, Nanocomplex, Sonication method, Antibacterial activity, Antifungal activity.

INTRODUCTION

The study of macrocyclic incorporated transition metal complexes derived from dioic and diamine has become increasingly interesting in chemistry due to the wide variety of applications in biological, analytical, medicinal, and industrial areas [1,2]. The metal binding to these macrocycles backbone is confined in the tetradentate, planar enclosed framework, which has unusual stability to the metal complex [3]. The chemistry of poly-azamacrocyclic complexes containing amide groups is an important area of research interest in the coordination chemistry of their ability to react with different metal ions to form stable complexes [4,5]. In the current era, nanocomplexes and nanomaterials have attracted much attention due to their distinctive applications in the chemical, optical, electrical, and biological fields [6-8]. The sonication technique for the synthesis of nanocomplexes emerged as an enchantment in the field of synthetic chemistry, arousing the area of sonication-assisted chemistry. Sonication-assisted synthesis involves sound waves penetrating inside the complexes and leading to uniformity in the reaction heating and a hundred times better speed, yield, and purity than conventional heating methods [9]. It is worth noting that the sonication technique is eco-friendly, offering better productivity, faster reactions, less solvent and energy [10].

Currently, antimicrobial resistance is growing globally and is the major concern to inhibit the growth of these microbes. Interest in transition metal-based drugs has gained attention in the field of bioinorganic chemistry due to their remarkable biological activity [11]. Transition metal macrocyclic complexes can exhibit remarkable antitumor, anticancer, antifungal,

and antibacterial activities [12,13]. Nanocomplexes of transition metals enhance antimicrobial activity by inhibiting microbial growth through a novel mechanism of action.

In present work, we have discussed the synthesis of a nanocomplex of Mn(II) using a macrocyclic ligand containing an amide group synthesized from the condensation of L-aspartic acid and *o*-phenylenediamine as precursors using conventional heating and sonication methods. In this context, the work purposes the synthesis, characterization and biological studies of nanocomplexes. The main aim of this work is the comparison of antimicrobial and antioxidative studies of the nanocomplex synthesized from two different protocols *viz*. conventional and sonication-assisted methods.

EXPERIMENTAL

All the solvents and chemicals used were of AR grade with high purity and further used without purification. L-Aspartic acid, *o*-phenylenediamine and manganese acetate were procured from Sigma-Aldrich (Germany) and used as such. The FT-IR spectra were measured in the solid-state using a Model Perkin -Elmer, which was operated in the wavenumber range of 4000-400 cm^{-1}. The CHNS elemental analysis was performed using Euro EA elemental analysis and the metal contents were estimated volumetrically. The molecular weight was determined by mass spectrometry using a Waters Q-Tof micromass (MS). The UV-vis absorption spectra were recorded using a Shimadzu spectrophotometer (UV-1800PC) and the wavelength range of 200-800 nm was employed. Field emission scanning electron microscopy (FE-SEM) images were taken on a Carl Supra 55. The EDS/EDX images were taken along with FE-SEM on Oxford Instruments software Aztec. The XRD pattern was taken on an X′Pert Pro XRD equipped with an X′celerator solid state detector and target copper with secondary monochromatic. The tested bacterial and fungal strains were purchased from the Institute of Microbial Technology, Chandigarh, India.

Synthesis of macrocyclic ligand

The macrocyclic ligand was synthesized using two different methods:

(A) Sonication-assisted method: The macrocyclic ligand was synthesized from equimolar quantities of L-aspartic acid (0.002 mol) and *o*-phenylenediamine (0.002 mmol) in 25 mL of ethanol in the presence of a few drops of conc. HCl and the reaction mixture were placed in a sonicator for 50 min at 70 ºC at a frequency of 40 kHz. The resulting product was washed and recrystallized from ethanol and finally dried under an IR lamp.

(B) Conventional method: In this method, the macrocyclic ligand was synthesized by the condensation reaction of a hot ethanolic solution (25 mL) of aspartic acid (0.002 mol) and a hot ethanolic solution (25 ml) of o-phenylenediamine (0.002 mol) mixed slowly with constant stirring. This mixture was refluxed at 70-80 ºC for 6-7 h in the presence of a few drops of conc. HCl. Upon cooling, the products obtained were then washed and recrystallized from ethanol and dried under an IR lamp. The schematic procedure is shown in **Scheme-I**.

Synthesis of Mn(II) nanocomplex

The Mn(II) nanocomplex was synthesized using sonication and a conventional method:

(A) Sonication-assisted method: In this method, a reaction mixture of manganese acetate (0.002 mol) and macrocyclic ligand (0.002 mmol) in 20 mL of ethanol in the presence of a few drops of conc. HCl was placed in a sonicator for 40 min at 60 ºC at a frequency of 40 kHz. The product was filtered, washed with ethanol, recrystallized from methanol and finally dried under an IR lamp.

(B) Conventional method: A solution of manganese acetate (0.002 mmol) in hot ethanol (20 mL) was added dropwise to a hot ethanolic solution (20 mL) of ligand (0.002 mol) with continuous stirring. The resulting solution was refluxed at 60-70 ºC for 5-6 h in the presence of a few drops of conc. HCl and placed overnight in a refrigerator. The product obtained was filtered, washed, recrystallized from ethanol, dried under an IR lamp, and ground manually in pestle mortar, so grinding was performed to obtain the complex in nano dimension. A schematic procedure is shown in **Scheme-II**.

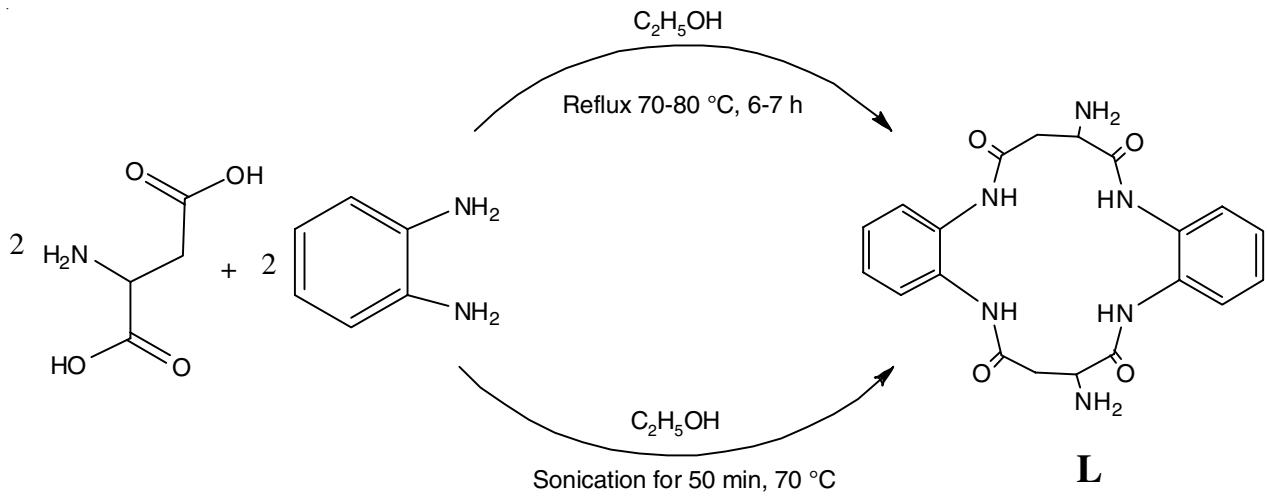

Scheme-I: Schematic representation of the synthesis of macrocyclic ligand L (7,18-diamino-7,8,17,18-tetrahydrodibenzo[b,j][1,4,9,12]-tetraazacyclohexadecine-6,9,16,19(5*H*,10*H*,15*H*,20*H*)-tetraone)

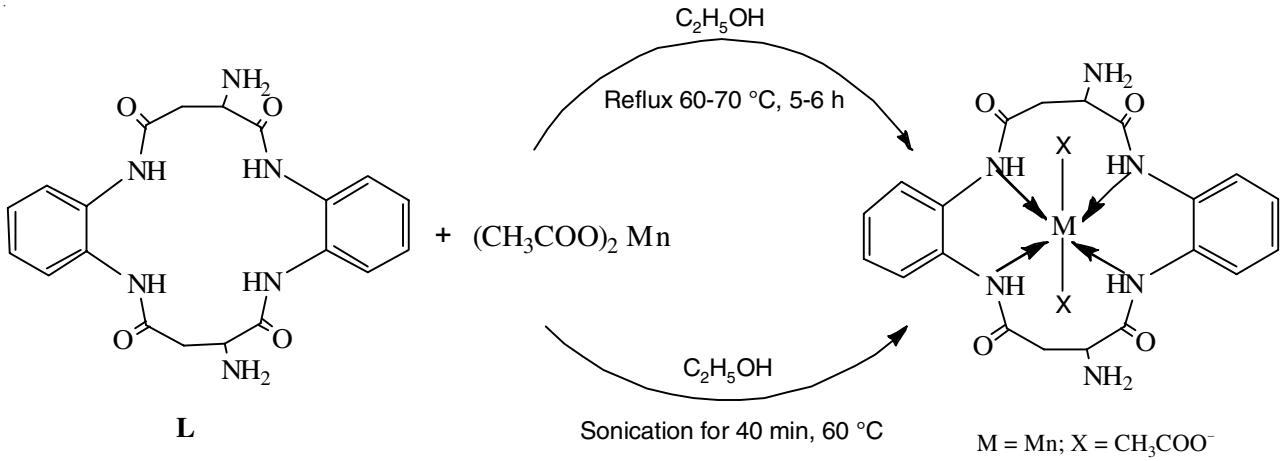

Scheme-II: Schematic representation of the synthesis of Mn(II) nanocomplex with macrocylic ligand L

Antimicrobial activity: The Mn(II) nanocomplexes were examined for their *in vitro* antibacterial activities against four Gram-positive bacteria, *i.e.* Staphylococcus aureus (MTCC No. 6845), *Enterococcus faecalis* (MTCC No. 441), *Bacillus subtilis* (MTCC No. 4214) and Listeria (MTCC No. 902), four Gram-negative bacteria, *Escherichia coli* (MTCC No. 448), *Salmonella enterica* (MTCC No. 1165), *Acinetobacter calcoaceticus* (MTCC No. 1948) and *Serratia marcescens* (MTCC No. 2645) and two fungal strains, i.e. *Aspergillus niger* (MTCC No. 9933) and *Candida albicans* (MTCC No. 227), using a standard two-fold serial dilution method in 96-well micro test plates. Chloromycin was used as a controlled drug for antibacterial activity and fluconazole was used for antifungal activity.

Biological assay: The minimal inhibitory concentration (MIC, µg/mL) is defined as the lowest concentration of target compounds that completely inhibit the growth of microbes [14]. To check the effect of solvent on microbial growth, DMSO was inoculated with microbes not treated with any medicine as a positive control. The microbial suspension was adjusted with sterile saline to a concentration of 1×10^5 CFU/mL. The stock solutions were prepared by dissolving complexes in DMSO solvent. The complexes and reference drugs were prepared in nutrient broth by twofold serial dilution to obtain the required concentrations of 800, 400, 200, 100, 50, 25, 12.5, 6.25, 3.125, and 1.56 µg/mL. These dilutions were incubated at 37 ± 2 ºC for 24 h. All bacterial and fungal growth was monitored visually and spectrophotometrically, and the experiments were performed in triplicate.

Antioxidant activity: The antioxidant activity of synthesized Mn(II) nanocomplexes was evaluated with the DPPH (2,2-diphenyl-1-picrylhydrazyl) method [15] and was recorded by measuring the change in the molar absorbance value of DPPH at 517 nm upon treatment with various concentrations. (25-100 µg/mL) in DMSO and ascorbic acid was used as a standard drug. A methanolic solution of DPPH (0.004%) was prepared. The stock solution for each complex was prepared in methanol (10 mg/10 mL), and further dilution was performed to prepare the required concentrations. Next, 2 mL of complex mixture was added to 1 mL DPPH-methanol solution. The resulting mixture was wrapped with aluminium foil and kept in the dark for 30 min. After 30 min, the scavenging activity was measured spectrophotometrically. The molar absorbance of DPPH-methanol solution used as a reference was observed at 517 nm using a UV-Vis spectrophotometer and the decrease in DPPH values of molar absorbance for different sample concentrations at 517 nm and change in colour of the solution from purple to colourless after reduction confirmed the DPPH radical scavenging by the antioxidant by donation of hydrogen radical or electron to form a stable DPPH-H molecule. The DPPH scavenging ability of the compounds was determined by the following equation:

$$\text{Inhibition of DPPH activity (\%)} = \frac{A_{control} - A_{sample}}{A_{control}} \times 100$$

where $A_{control}$ is the absorbance of the control (reference) and A_{sample} is the absorbance of the sample.

RESULTS AND DISCUSSION

The Mn(II) nanocomplex was synthesized by using two different methods, *i.e.* sonication-assisted and conventional methods. The sonication method increased the yield of the final product with reduced reaction time, enhanced purity and less solvent. The comparison data between the two methods is tabulated in Table-1.

The elemental analysis results of the macrocyclic ligand and its Mn(II) nanocomplex agreed with their empirical formulae as shown in Table-2. The ligand and its Mn(II) complexes were reacted in a 1:1 stoichiometry, which indicates the form-

TABLE-1
COMPARISON BETWEEN SONICATION AND CONVENTIONAL METHODS

Complexes	Reaction period		Solvent (mL)		Yield (%)	
	Sonication (min)	Conventional (h)	Sonication (min)	Conventional (h)	Sonication (min)	Conventional (h)
$C_{20}H_{22}N_6O_4$	50.0	6.5	25.0	50.0	85	63
$C_{24}H_{28}N_6O_8Mn$	40.0	5.5	20.0	40.0	88	70

TABLE-2
ANALYTICAL AND PHYSICAL DATA RECORDED FOR ALL SYNTHESIZED NANO COMPLEX

Complexes	Colour	Melting point (°C)	Elemental analysis (%): Found (calcd.)			
			C	H	N	Mn
$C_{20}H_{22}N_6O_4$	Creamy white	196-198	56.01 (58.53)	5.29 (5.40)	20.40 (20.48)	–
$C_{24}H_{28}N_6O_8Mn$	Light brown	251-253	48.99 (49.41)	4.80 (4.84)	14.29 (14.40)	9.33 (9.42)

ation of mononuclear complexes. The complexes formed are solid, coloured and air-stable at room temperature. All the complexes were soluble in common organic solvents, such as DMSO and DMF but insoluble in ethanol, methanol, acetone, hexane, chloroform and both hot and cold water.

FT-IR studies: The FT-IR absorption bands provided information about the mode of coordination in the synthesized complexes. In the FT-IR spectrum of the macrocyclic ligand (Fig. 1), the characteristic band at 3169 cm^{-1} can be assigned to the stretching vibration of ν(N-H), and the appearance of three bands in the regions of 1643, 1250, and 681 cm^{-1} could be assigned to the three different modes of the amide group, suggesting the formation of the closed macrocyclic enclosed region [16]. For the Mn(II) complex (Fig. 2), the ν(N-H) band shifts to a lower frequency of 3158 cm^{-1}. The appearance of three bands in the regions of 1634, 124,5, and 661 cm^{-1} could be assigned to the three different modes of the amide group, and a strong band at 515 cm^{-1} appeared in the metal complex

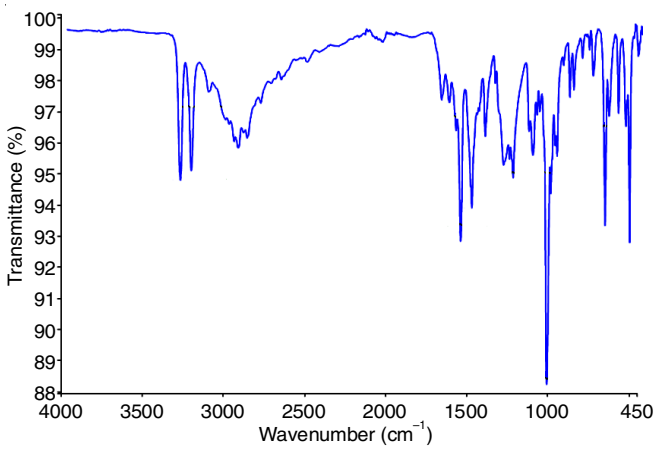

Fig. 1. FT-IR spectra of macrocyclic ligand (L)

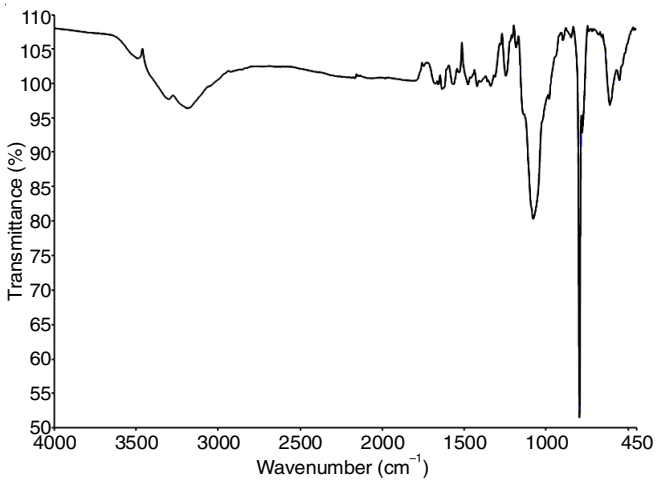

Fig. 2. FT-IR spectra of Mn(II) nano complex

corresponding to the M-N vibration, indicating that the coordination of the metal occurs through the nitrogen atom of the amide group in the macrocyclic complex [17].

UV-Vis studies: The UV-Vis spectra of the Mn(II) nanocomplex were recorded in DMSO solvent (Fig. 3). It exhibits a strong *d-d* band at approximately 540 nm assignable to $^6A_{1g} \rightarrow {}^4T_{1g}$, suggesting an octahedral geometry and a band at approximately 334 nm transitions can be attributed to the π-π* transition and a band at approximately 260 nm due to intra-ligand charge transfer [6].

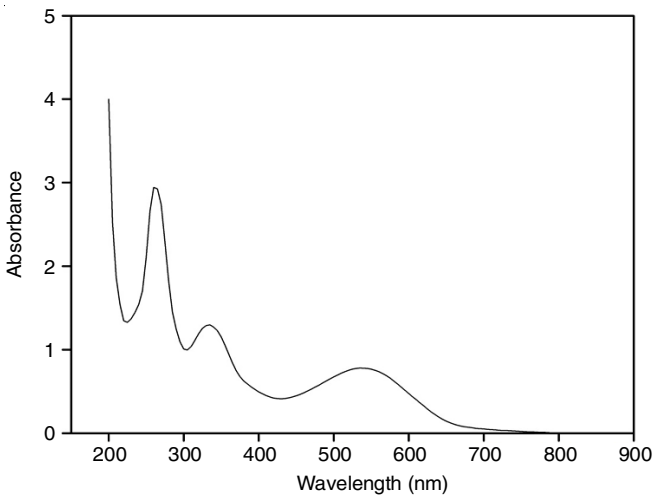

Fig. 3. UV-vis spectra of the Mn(II) complex

Mass studies: The Mass spectra of the macrocyclic ligand and Mn(II) complex were studied at room temperature. The mass spectrum of macrocyclic ligand L (Fig. 4) shows a peak at *m/z* = 410.38, which is in good agreement with its formula molecular weight (410.43). The mass spectrum of the Mn(II) nanocomplex (Fig. 5) shows a peak at *m/z* = 587.03 for the molecular ion peak, which is very close to its formula molecular weight (587.17) and the base peak was observed at *m/z* 212.62.

EPR studies: The solid-state EPR spectrum of the nanocomplex was recorded at room temperature at an X-band frequency of 9.719 GHz. The ESR spectra (Fig. 6) of Mn(II) in a solid-state at room temperature show a strong signal centered at g = 2, which is associated with an I = 5/2 nuclear spin of ^{55}Mn, confirming that Mn(II) ions are in an environment close to the octahedral geometry [18].

XRD studies: Fig. 7 shows the X-ray powder diffraction pattern of Mn(II) nanocomplexes synthesized by two different methods *i.e.* sonication-assisted and conventional methods. The data were recorded by using Cu*K*α radiation. The intensity data were collected over a range of 5-80º. The average crystalline

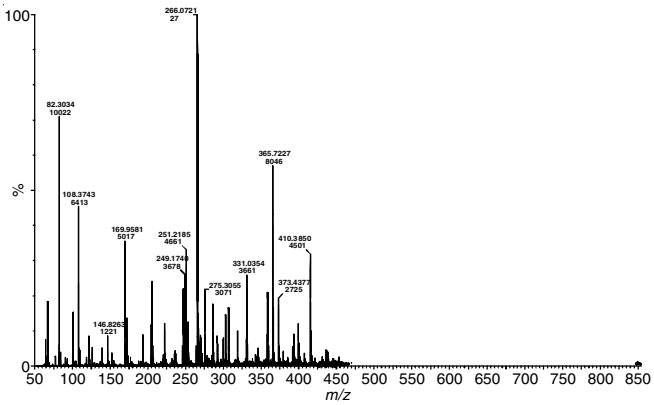

Fig. 4. Mass spectra of macrocyclic ligand (L)

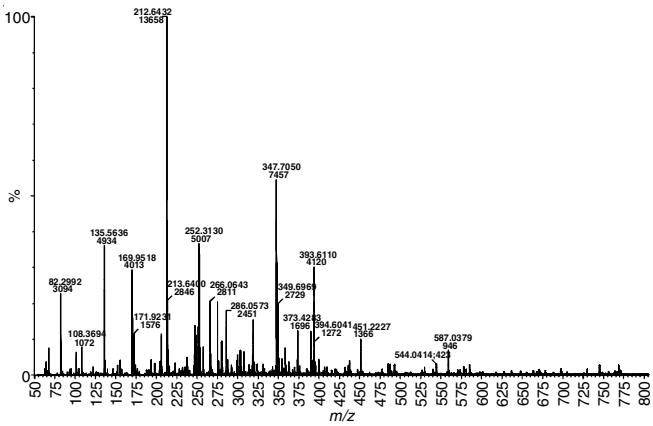

Fig. 5. Mass spectrum of the Mn(II) complex

Fig. 6. EPR spectrum of the Mn(II) complex

size of the nanocomplexes was estimated with the Debye-Scherrer's equation (eqn. 1):

$$D = \frac{K\lambda}{\beta\cos\theta} \quad (1)$$

where D is the average crystallite size in nm, β is the breadth of the observed diffraction line at its half-maximum intensity, K is the shape factor, which usually has a value of 0.89, λ = 0.15406 nm, is the wavelength of the X-ray radiation and θ is the corresponding incidence angle [19]. The average crystalline sizes of the Mn(II) nanocomplex synthesized by sonication and the conventional method were found to be 42.29 and 85.63

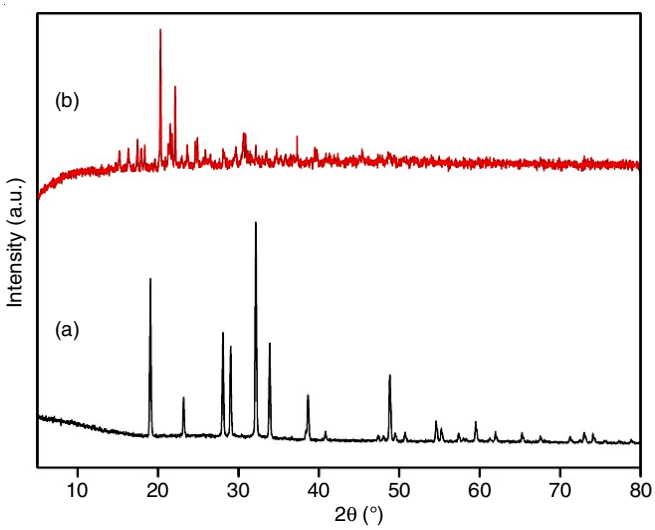

Fig. 7. XRD pattern of Mn(II) nanocomplex synthesized by (a) sonication-assisted method and (b) conventional heating method showed that complexes formed by (a) is better

nm, respectively. The crystalline area found in the sonication-assisted method was greater than that in the conventional heating method due to rapid micromixing during sonication. A well-defined nanocomplex was formed in less time. On the other hand, the less crystalline nature of Mn(II) nanocomplexes formed by the conventional method could be because the complex was exposed for a longer duration of time in comparison to the sonication method. Fig. 7 shows that sonication irradiation significantly decreased the size of the Mn(II) complexes compared to the conventional method. The unit cell parameters were calculated using the hit and trial method and matched with JCPDF card no. and found to be hexagonal for Mn(II) nanocomplexes with unit cell parameters $a = 5.2350$ Å, $b = 5.2350$ Å, $c = 9.9610$ Å, $\alpha=\beta= 90^\circ$ and $\gamma =120^\circ$.

FE-SEM studies: The morphologies of the synthesized Mn(II) nanocomplexes by two different methods was investigated by FE-SEM and the results are depicted in Fig. 8. The FE-SEM image for the Mn(II)nanocomplex synthesized by the conventional method (Fig. 8a), depicts the formation of nanosized particles with irregular morphology, whereas that of sonication irradiation depicted in Fig. 8b shows that the size of the complex was reduced and obtained without any agglomeration. It is concluded that the sonication irradiation method facilitates the formation of Mn(II) nanocomplex, which provides an improved surface morphology when compared to the conventional heating method.

Antimicrobial assay: In present study, the antimicrobial study of macrocyclic ligand and its Mn(II) nanocomplex synthesized by two different methods were tested against four Gram-positive (*Staphylococcus aureus*, *Enterococcus faecalis*, *Bacillus subtilis*, *Listeria*), four Gram-negative bacteria (*Escherichia coli*, *Salmonella enterica*, *Acinetobacter calcoaceticus*, *Serratia marcescens*) and two fungal strains (*Aspergillus niger*, *Candida albicans*). The results revealed that the nanocomplex obtained from the sonication method exhibited powerful antimicrobial activity compared to those nanocomplex synthesized by the conventional method (Tables 3a-b and 4).

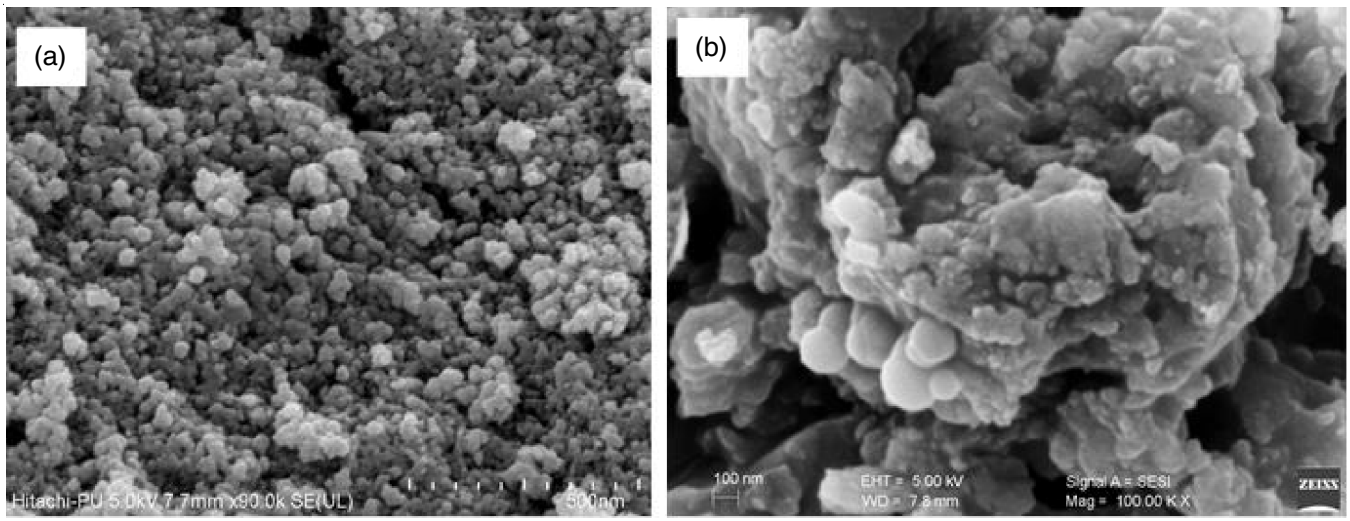

Fig. 8. FE-SEM images of Mn(II) nano complexes synthesized by (a) sonication-assisted method and (b) conventional heating method

TABLE-3a
COMPARATIVE ANALYSIS OF GRAM-POSITIVE BACTERIAL SCREENING OF SYNTHESIZED COMPLEXES (EXPRESSED AS MIC IN µg/mL)

Complexes	*Enterococcus faecalis*		*Bacillus subtilis*		*Listeria sp.*		*Staphylococcus aureus*	
	Sonication	Conventional	Sonication	Conventional	Sonication	Conventional	Sonication	Conventional
$C_{20}H_{22}N_6O_4$	200	400	100	400	200	400	200	400
$C_{24}H_{28}N_6O_8Mn$	1.56	25	25	50	6.25	25	1.56	25
Chloromycin	3.125		1.56		1.56		3.125	

TABLE-3b
COMPARATIVE ANALYSIS OF GRAM-NEGATIVE BACTERIAL SCREENING OF SYNTHESIZED COMPLEXES (EXPRESSED AS MIC IN µg/mL)

Complexes	*Escherichia coli*		*Salmonella enterica*		*Acinetobacter calcoacetius*		*Serratia marcescens*)	
	Sonication	Conventional	Sonication	Conventional	Sonication	Conventional	Sonication	Conventional
$C_{20}H_{22}N_6O_4$	200	400	400	400	200	400	200	400
$C_{24}H_{28}N_6O_8Mn$	50	125	100	400	50	200	50	200
Chloromycin	3.125		50		3.125		1.56	

TABLE-4
COMPARATIVE ANALYSIS OF FUNGAL SCREENING OF SYNTHESIZED COMPLEXES (EXPRESSED AS MIC IN µg/mL)

Complexes	*C. albicans*		*Aspergillus niger*	
	Sonication	Conventional	Sonication	Conventional
$C_{20}H_{22}N_6O_4$	100	400	200	400
$C_{24}H_{28}N_6O_8Mn$	6.25	25	25	50
Fluconazole	1.56		25	

This is attributed to the reduced size and even morphology of Mn(II)nanocomplex obtained from the sonication method, which enhanced their reactivity and activity to kill microbial growth by deeply intervening with the cell wall, resulting in altered cell permeability and leading to cell death [20].

However, the antimicrobial activity of the nanocomplexes can be explained by overtone's concept and chelation theory [21]. As per the theory, the polarity of the transition metal ion reduces due to chelation, the partial sharing of its positive charge with the donor groups in the cyclic background of the macrocycle and π-electron delocalization over the whole chelation ring, which increases the lipophilic character of the macrocyclic complex and subsequently plays a role in the metabolic pathways of these microbes [22].

Antioxidant activity: The antioxidant activities of the macrocyclic ligand and its Mn(II) nanocomplexes were synthesized by two different methods were performed by the DPPH scavenging method. Table-5 shows the inhibitory effects of macrocyclic ligand (L) and its nanometal complexes on the DPPH radical. The inhibitory effects of the tested complexes against the DPPH radical were observed in an increasing dose-dependent manner, and the suppression ratio increased with increasing concentrations (25-100 µg/mL) of the complexes using ascorbic acid as a reference. The data revealed that the

TABLE-5
ANTIOXIDANT ACTIVITY IN TERMS OF CONCENTRATION ON SCAVENGING ACTIVITY (%) OF MACROCYCLIC LIGAND AND ITS Mn(II) NANO COMPLEXES

Conc. (µg/mL)	$C_{20}H_{22}N_6O_4$		$C_{24}H_{28}MnN_6O_8$		Ascorbic acid
	Sonication	Conventional	Sonication	Conventional	
25	23.8	39.1	34.0	52.8	60.0
50	26.5	42.5	35.6	57.6	63.3
75	30.2	45.8	39.0	62.7	68.2
100	35.8	48.9	42.8	65.7	70.7

Mn(II) nanocomplex synthesized by the sonication method showed better DPPH radical scavenging activity than that synthesized by the conventional heating method.

Conclusion

In present work, the comparative analysis of the sonication assisted and conventional synthesis of Mn(II) nanocomplex was conducted in order to investigate the better biological potency. The synthesized complexes were characterized using different techniques such as FT-IR, electronic spectra, mass spectra, ESR, FE-SEM and X-ray diffraction. Based on the spectral data, it is confirmed that the metal complex possesses an octahedral geometry and FE-SEM images revealed the regular morphology of the nanocomplex synthesized from the sonication method compared with the conventional method. The antimicrobial screening data obtained against different bacterial and fungal strains indicated the enhanced activity of nanocomplex from the sonication method. Hence, the Mn(II) nanocomplex synthesized by a sonication method could be a better material for biological applications.

ACKNOWLEDGEMENTS

The authors are grateful to CSIR, New Delhi, India for financial help in the form of a junior research fellowship (JRF) (file No. 09/140(0180)/2020-EMR-I) and to authorities of Thapar Institute of Engineering and Technology, Patiala, India for providing necessary research facilities.

CONFLICT OF INTEREST

The authors declare that there is no conflict of interests regarding the publication of this article.

REFERENCES

1. G. Grivani, A. Ghavami, M. Kuèeráková, M. Dusek and A.D. Khalaji, *J. Mol. Struct.*, **1076**, 326 (2014); https://doi.org/10.1016/j.molstruc.2014.07.073
2. S. Rani, S. Kumar and S. Chandra, *Spectrochim. Acta A Mol. Biomol. Spectrosc.*, **118**, 244 (2014); https://doi.org/10.1016/j.saa.2013.08.079
3. H.A. El-Boraey and O.A. EL-Gammal, *J. Incl. Phenom. Macrocycl. Chem.*, **90**, 123 (2018); https://doi.org/10.1007/s10847-017-0774-9
4. N. Sharma, D. Kumar, R. Shrivastava, S. Shrivastava and K.K. Awasthi, *Mater. Today Proc.*, **42**, 1760 (2021); https://doi.org/10.1016/j.matpr.2020.12.1225
5. D. Kumar, N. Sharma and M. Nair, *J. Biol. Inorg. Chem.*, **22**, 535 (2017); https://doi.org/10.1007/s00775-017-1440-9
6. O.B. Ibrahim, M.A. Mohamed and M.S. Refat, *Can. Chem. Trans.*, **2**, 108 (2014).
7. V. Sangwan and D.P. Singh, *J. Chin. Chem. Soc.*, **67**, 592 (2020); https://doi.org/10.1002/jccs.201900139
8. Z. Parsaee and K. Mohammadi, *J. Mol. Struct.*, **1137**, 512 (2017); https://doi.org/10.1016/j.molstruc.2017.02.026
9. A.H. Ismail, H.K. Al-Bairmani, Z.S. Abbas and A.M. Rheima, *IOP Conf. Series: Mater. Sci. Eng.*, **928**, 052028 (2020); https://doi.org/10.1088/1757-899X/928/5/052028
10. M.A. Bakht, *Life Sci.*, **10**, 79 (2015).
11. N. Zare, A. Zabardasti, A. Mohammadi, A. Kakanejadifard and F. Azarbani, *J. Iran. Chem. Soc.*, **16**, 1501 (2019); https://doi.org/10.1007/s13738-019-01626-1
12. M. Bouhdada, M. EL Amane, B.B. Mohammed and K. Yamni, *J. Mol. Struct.*, **1177**, 391 (2019); https://doi.org/10.1016/j.molstruc.2018.09.047
13. H.A. El-Boraey, M.A. El-Salamony and A.A. Hathout, *J. Incl. Phenom. Macrocycl. Chem.*, **86**, 153 (2016); https://doi.org/10.1007/s10847-016-0649-5
14. H.B. Liu, W.W. Gao, V.K.R. Tangadanchu, C.H. Zhou and R.X. Geng, *Eur. J. Med. Chem.*, **143**, 66 (2018); https://doi.org/10.1016/j.ejmech.2017.11.027
15. P. Kavitha, M. Saritha and K.L. Reddy, *Spectrochim. Acta A Mol. Biomol. Spectrosc.*, **102**, 159 (2013); https://doi.org/10.1016/j.saa.2012.10.037
16. P. Gull, M.A. Malik, O.A. Dar and A.A. Hashmi, *Microb. Pathog.*, **104**, 212 (2017); https://doi.org/10.1016/j.micpath.2017.01.036
17. U. Kumar and S. Chandra, *J. Saudi Chem. Soc.*, **15**, 187 (2011); https://doi.org/10.1016/j.jscs.2010.08.002
18. Y. Abdi, N. Bensouilah, D. Siziani, M. Hamdi, A.M. Silva and B. Boutemeur-Kheddis, *J. Mol. Struct.*, **1202**, 127307 (2020); https://doi.org/10.1016/j.molstruc.2019.127307
19. A.A. Fahem, *Spectrochim. Acta A Mol. Biomol. Spectrosc.*, **88**, 10 (2012); https://doi.org/10.1016/j.saa.2011.11.037
20. A. Singh and A. Chaudhary, *J. Iran. Chem. Soc.*, **17**, 973 (2020); https://doi.org/10.1007/s13738-019-01829-6
21. N. Fahmi, I. Masih and K. Soni, *J. Macromol. Sci. A*, **52**, 548 (2015); https://doi.org/10.1080/10601325.2015.1039334
22. N. Bensouilah, B. Boutemeur-Kheddis, H. Bensouilah, I. Meddour and M. Abdaoui, *J. Incl. Phenom. Macrocycl. Chem.*, **87**, 191 (2017); https://doi.org/10.1007/s10847-016-0690-4